Acellular Hydrogels for Regenerative Burn Wound Healing: Translation from a Porcine Model

Yu-I Shen[1,5], Hyun-Ho G. Song[1,5], Arianne E. Papa[2], Jacqueline A. Burke[2], Susan W. Volk[3] and Sharon Gerecht[1,4]

Currently available skin grafts and skin substitutes for healing following third-degree burn injuries are fraught with complications, often resulting in long-term physical and psychological sequelae. Synthetic treatment that can promote wound healing in a regenerative manner would provide an off-the-shelf, non-immunogenic strategy to improve clinical care of severe burn wounds. Here, we demonstrate the vulnerary efficacy and accelerated healing mechanism of a dextran-based hydrogel in a third-degree porcine burn model. The model was optimized to allow examination of the hydrogel treatment for clinical translation and its regenerative response mechanisms. Hydrogel treatment accelerated third-degree burn wound healing by rapid wound closure, improved re-epithelialization, enhanced extracellular matrix remodeling, and greater nerve reinnervation, compared with the dressing-treated group. These effects appear to be mediated through the ability of the hydrogel to facilitate a rapid but brief initial inflammatory response that coherently stimulates neovascularization within the granulation tissue during the first week of treatment, followed by an efficient vascular regression to promote a regenerative healing process. Our results suggest that the dextran-based hydrogels may substantially improve healing quality and reduce skin grafting incidents and thus pave the way for clinical studies to improve the care of severe burn injury patients.

Journal of Investigative Dermatology (2015) **135,** 2519–2529; doi:10.1038/jid.2015.182; published online 25 June 2015

INTRODUCTION

In 2013, ~450,000 burn injuries received medical treatment (Stoddard *et al.*, 2014), and the estimated hospital care cost in high-income countries is estimated to exceed US$88,000 per burn patient (Hop *et al.*, 2014). Survival in the most severely burned patients is often accompanied by orthopedic, neurologic, metabolic complications, and significant psychosocial challenges brought about by poor healing and excessive scar formation (Stoddard *et al.*, 2014). Therefore, challenges remain to improve serious burn wound healing. Unlike superficial burn wounds that can heal on their own without advanced professional care, third-degree burns, which are characterized by full-thickness damage of the skin, most often require surgical intervention and replacement of damaged skin with skin grafts or skin substitutes (Sheridan, 2012). Biomaterials that are able to induce a regenerative healing response would therefore promise significant improvement in clinical care and long-term outcomes of wound patients, particularly those sustaining burn injury.

Porcine wound healing is considered to be most similar to that of humans, and as a translational model pigs display the greatest concordance with human trials (Sullivan *et al.*, 2001). First, porcine skin most closely resembles human skin both anatomically and physiologically. Both have similar dermal–epidermal thickness ratios and dermal vascularization patterns (Sullivan *et al.*, 2001; Middelkoop *et al.*, 2004). Biochemically, porcine and human skin have similar collagen matrix and keratinous proteins (Singer and McClain, 2003). Studies have also shown an excellent agreement between pig and human with respect to wound healing responses from growth factors (Sullivan *et al.*, 2001). Despite these benefits, technical difficulties limit the use of pig models for studies of third-degree burns. Indeed, unlike superficial burn wounds, which can easily be created using accessible tools and temperatures, there is limited literature on modeling severe burn injuries in a reproducible manner and on the criteria for assessing the healing kinetics, especially for the purpose of evaluating biomaterials.

Our laboratory has developed an acellular dextran-based hydrogel, dextran-allyl isocyanate-ethylamine, that is tailored to promote rapid neovascularization and has been proven to accelerate third-degree burn healing with complete skin

[1]*Department of Chemical and Biomolecular Engineering, Johns Hopkins Physical Sciences—Oncology Center and Institute for NanoBioTechnology, Johns Hopkins University, Baltimore, Maryland, USA;* [2]*Department of Biomedical Engineering, Johns Hopkins University, Baltimore, Maryland, USA;* [3]*Department of Clinical Studies—Philadelphia, University of Pennsylvania School of Veterinary Medicine, Philadelphia, Pennsylvania, USA and* [4]*Department of Materials Science and Engineering, Johns Hopkins University, Baltimore, Maryland, USA*

Correspondence: Sharon Gerecht, Department of Chemical and Biomolecular Engineering, Johns Hopkins Physical Sciences—Oncology Center and Institute for NanoBioTechnology, Johns Hopkins University, 3400 North Charles Street, Baltimore, Maryland 21218, USA. E-mail: gerecht@jhu.edu

[5]*The first two authors contributed equally to this work.*

Received 18 November 2014; revised 9 April 2015; accepted 23 April 2015; accepted article preview online 8 May 2015; published online 25 June 2015

© 2015 The Society for Investigative Dermatology

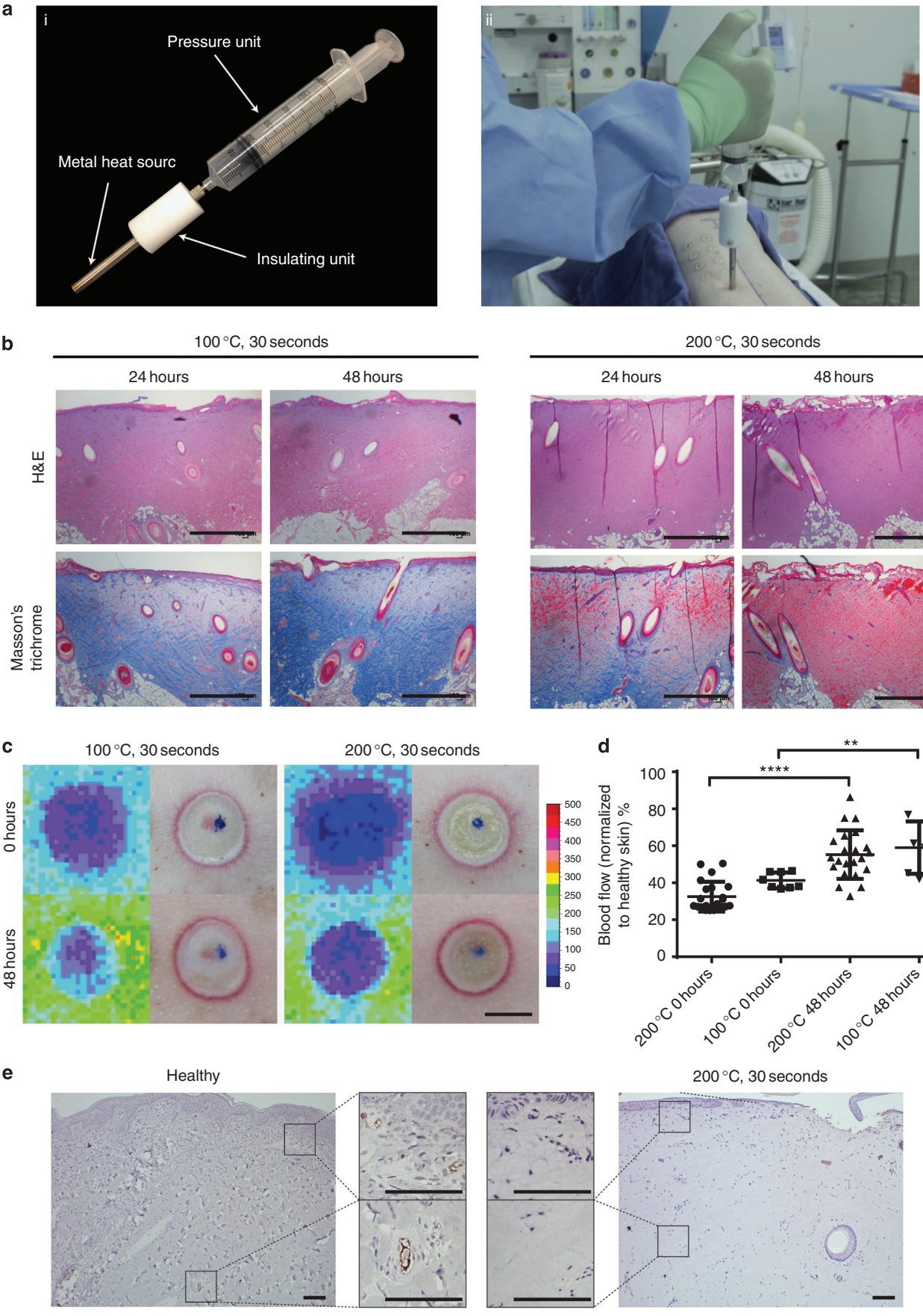
a
i
Pressure unit
Metal heat sourc
Insulating unit
ii
b
100 °C, 30 seconds
200 °C, 30 seconds
24 hours
48 hours
24 hours
48 hours
H&E
Masson's trichrome
c
100 °C, 30 seconds
200 °C, 30 seconds
0 hours
48 hours
500
450
400
350
300
250
200
150
100
50
0
d
**
****
Blood flow (normalized to healthy skin) %
100
80
60
40
20
0
200 °C 0 hours
100 °C 0 hours
200 °C 48 hours
100 °C 48 hours
e
Healthy
200 °C, 30 seconds

regeneration in a murine model (Sun *et al.*, 2010, 2011). The present study tested the efficacy and mechanism by which dextran hydrogels promote regenerative healing in a third-degree porcine burn wound model.

RESULTS

Dextran-based hydrogels for third-degree burn wounds in pigs

We generated dextran-based hydrogels modified with allyl isocyanate and ethylamine functional groups and crosslinked with polyethylglycol diacrylate (Sun *et al.*, 2010, 2011). To investigate the safety and efficacy action mechanism of the dextran-based hydrogel in the porcine third-degree burn injury model, we designed a custom-made device inspired from a previous study (Branski *et al.*, 2008). This device is comprised of three parts, including a metal heat source, insulation units, and pressure units (Figure 1ai), allowing for reproducible delivery of the temperature, the duration of the contact with the object, and the pressure.

To create the wounds, the device was held at a 90° angle to the skin with a constant pressure of 2 kg cm^{-2} (Figure 1aii). As significant thermal insult is associated with progressive injury to deep tissues compared with superficial damage until 48 hours after injury (Papp *et al.*, 2004), the degree of burn damage was evaluated in wounds 24 or 48 hours after the burn (Branski *et al.*, 2008; Gaines *et al.*, 2013). Healthy porcine skin tissue sections are shown in Supplementary Figure 1 online. To induce full-thickness dermal injury, a heat source of 200 °C, applied for 30 seconds, was required (Figure 1b). In contrast, application of a heat source of 100 °C for either 30 or 60 seconds caused injury to the superficial dermis but did not reliably cause full-thickness (third-degree) burn injury (Figure 1b; data not shown). As anticipated, evidence of dermal injury progressed between 24 and 48 hours. Thus, the use of 200 °C for 30 seconds was chosen to generate third-degree burns in assessing the ability of the dextran-based hydrogel to improve healing of burn wounds. The significant damage induced by thermal injury in this model is also evidenced by the reduction in blood flow, indicating more severe damage to blood vessels (Figure 1c and d) and the lack of blood vessels throughout the depth of the injured dermis 48 hours after application of the 200 °C for 30 seconds (Figure 1e).

Vascular ingrowth, maturation, and regression in hydrogel-treated burn wounds

Following excision of the necrotic tissue after 48 hours, hydrogels were applied as skin substitutes. Because complete excision of the avascular zone of coagulation has been shown to improve outcomes when biomaterials are used for burn wound treatment, we investigated whether it was necessary for maximal efficacy to resect beyond the original injury site (complete) or whether a more conservative resection (partial) would be sufficient. In the first protocol, we followed the approach used in our previously published murine burn model in which a 1.2 cm diameter biopsy punch was used to excise the burn wound made by a 1.2 cm diameter stainless-steel device (Sun *et al.*, 2011) and excised the entire initial contact site of the thermal burn. The excised areas were then treated with pre-crosslinked hydrogels shaped to fit the size of the wounds. In the second protocol, all the necrotic tissue samples were excised, up to 3 mm in diameter beyond the initial contact site (Supplementary Movie 1 online).

Immunohistochemical staining for CD31 was seen by day 5 only in wounds that had complete excision of the burn wound. In contrast, incomplete excision negatively impacted vascularization of the hydrogel during that time frame (Figure 2a). Hydrogel vascularization, quantified both as vessel density and the percentage of area covered by the vessels 2 weeks after treatment, confirmed a more efficient vascularization followed by vascular regression for the completely excised wounds, consistent with a superior healing process (Figure 2b), prompting selection of this model for use in all subsequent studies.

We next examined the ability of the hydrogel to promote vascularization and subsequent vessel regression within healing wounds compared with wounds treated with dressing alone following complete excision of burn injured tissue. In the first week after excision, mean vascular density in both groups was increased at both days 5 and 7 when compared with baseline. However, a more rapid vascular regression was noted in hydrogel-treated wounds. Specifically, the hydrogel-treated wounds exhibited a significant decrease in vessel density by day 14, whereas the dressing-only–treated group showed no significant change over the same time period (Figure 2c). Blood flow analysis on day 14 confirmed a significant reduction in blood flow in the hydrogel-treated wounds compared with blood flow analysis of dressing-only–treated wounds, which was closer to that seen in uninjured skin (Figure 2d), supporting hydrogel-induced resolution of the initial vascular phase of wound repair.

Wound closure and re-epithelialization

A key feature of any healed wound is complete re-epithelialization. We have examined dressing versus hydrogel treatment. Occasionally, dressing change interrupted the integrity of the healing area, which prompted us to also examine the re-debridement on day 5 followed by re-application of hydrogel or dressing-only. Gross examination of the wounds at day 14 revealed a delay in wound closure in the dressing-only–treated wounds compared with hydrogel-treated wounds (Figure 3ai).

Examining gross wound closure, we found that all hydrogel-treated wounds appeared closed, whereas just 14% of dressing-only–treated wounds and none of the

Figure 1. Induction of third-degree burn injury in pigs. (**a**) (i) A custom-made burn device is held upright on the (ii) pig's thoracic paravertebral zone. (**b**) Representative images of hematoxylin and eosin (H&E) and Masson's trichrome histological stains of the wounds at different temperatures and burn durations. (**c**) Laser speckle contrast images with their corresponding wound photographs and (**d**) quantification of blood flow in healthy skin and burn wounds. $N = 22$ and 8 for 200 °C and 100 °C, respectively. (**e**) Immunohistochemistry for CD31 of the 200 °C, 30 seconds. Forty-eight hours show no vessels in the wounded area compared with healthy skin. Significance levels were set at $^{**}P < 0.01$, and $^{****}P < 0.0001$. Bars = 1 mm in **b**, 1 cm in **c**, and 100 μm in **e**.

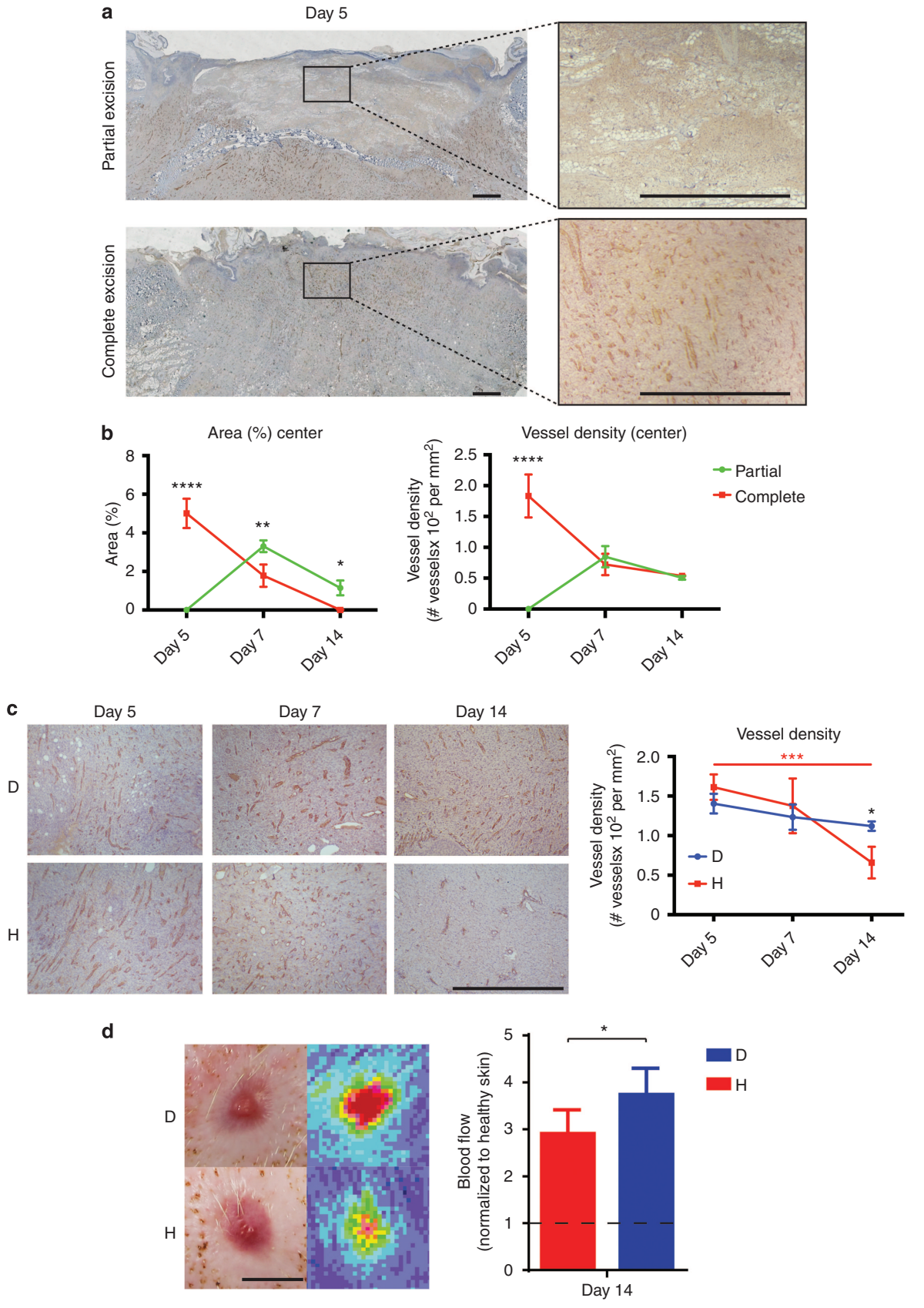
a
Day 5
Partial excision
Complete excision
b
Area (%) center
Area (%)
Day 5
Day 7
Day 14
Vessel density (center)
Vessel density (# vesselsx 10² per mm²)
Partial
Complete
c
Day 5
Day 7
Day 14
D
H
Vessel density
Vessel density (# vesselsx 10² per mm²)
d
Blood flow (normalized to healthy skin)
Day 14

dressing-retreated wounds were closed (Figure 3aii), resulting in wound gap in the dressing-only–treated wounds and a larger gap in the dressing-retreated wounds (Figure 3aiii). Although all hydrogel-treated wounds closed on day 14, there was a delay in the dressing-only–treated wounds. Identification of the neoepithelium on Masson's trichrome or K14 (keratinocyte marker)-stained sections confirmed that dressing-only–treated wounds had an epithelial gap, whereas hydrogel-treated wounds were completely re-epithelialized (Figure 3b). A similar trend was found with retreated wounds, where dressing-only–retreated wounds had a gap in the epithelial layer, whereas hydrogel-retreated wounds were closed with a thick and reticulated epithelial layer (Figure 3c). Correspondingly, dressing-only–retreated wounds were only about 50% re-epithelialized compared with hydrogel-retreated wounds, which were all completely re-epithelialized ($P<0.01$). A similar trend was seen for hydrogel single application versus dressing-alone control. We next quantified the rete ridges percentage (i.e., the percent of the reticulated epithelium in the regenerated epithelium) and the rete ridges (Kiwanuka *et al.*, 2011). We found that dressing-only–treated wounds had a very low rete ridges percentage and density, whereas hydrogel-treated and -retreated wounds exhibited high rete ridges percentage and rete ridges density. Consistent with a superior regenerative response, hydrogel-treated wounds have a rete ridges density similar to that of healthy skin (Figure 3i–ii). Finally, the hydrogel-treated and -retreated wounds exhibited a similar decrease in vessel

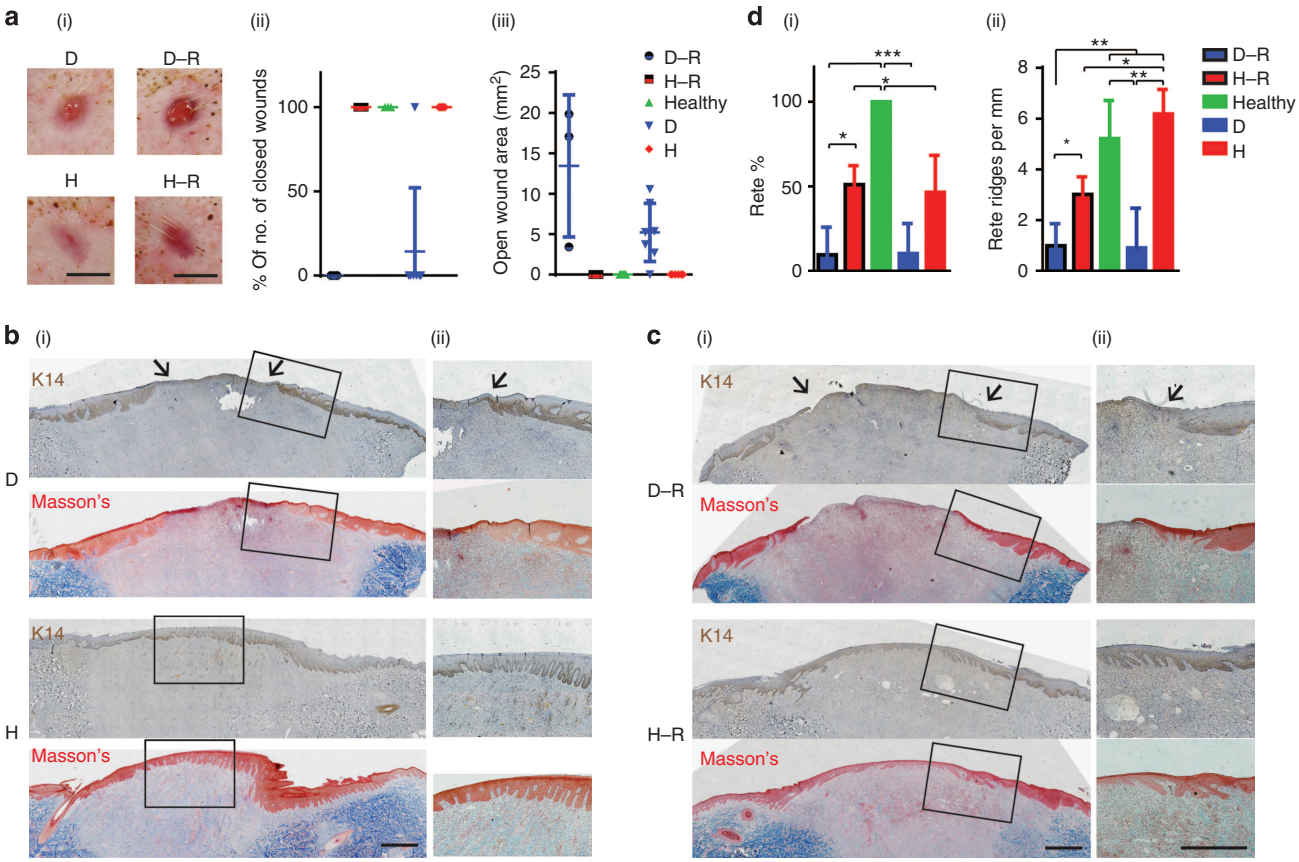

Figure 3. Wound closure and re-epithelialization. (**a**) Wounds on day 14: (i) representative wound images; (ii) percentage closed wounds gap, and (iii) open wound area. $N=7$ for D and H and $N=3$ for D–R and H–R. (**b** and **c**) Wounds on day 14: (i) representative wound images and (ii) immunohistochemistry for K14 (upper panel; arrows indicate open wound) and Masson's trichrome stain (lower panel). High magnifications of the boxed areas are shown on the right. (**c**) Wounds on day 14. (**d**) Quantification of (i) rete percentage and (ii) rete density of day 14–treated wound. $N=3$. Bars = 1 cm in **a**i and **b**i; 1 mm in **a**ii and **b**ii; and 0.5 mm in high magnification insets. Significance levels were set at $^{*}P<0.05$, $^{**}P<0.01$, and $^{***}P<0.001$. D, dressing-only–treated wound; D–R, dressing-retreated wound; H, hydrogel-treated wound; H–R, hydrogel-retreated wound.

Figure 2. Wound excitement and kinetics of vascularization. (**a**) Immunohistochemistry for CD31 of wound area depicting vascular ingrowth on day 5 for partially excised (method 1) and completely excised (method 2). High magnifications of the boxed areas are shown on the right. (**b**) Quantification of CD31 stains of the wounds treated in both methods over 2 weeks. $N=3$ per time point. (**c**) CD31 and quantification of vasculature over 2 weeks of the wounds. $N=3$ per time point. (**d**) Laser speckle contrast images (right) and quantification (left) of blood flow on day 14. $N=7$. Bars = 1 mm in **a** and **c** and 1 cm in **d**. Red asterisks indicate a significant change along time; black asterisk indicates a significant difference between the two treatments at a given time point. Significance levels were set at $^{*}P<0.05$, $^{**}P<0.01$, $^{***}P<0.001$, and $^{****}P<0.0001$. D, dressing-only–treated wound; H, hydrogel-treated wound.

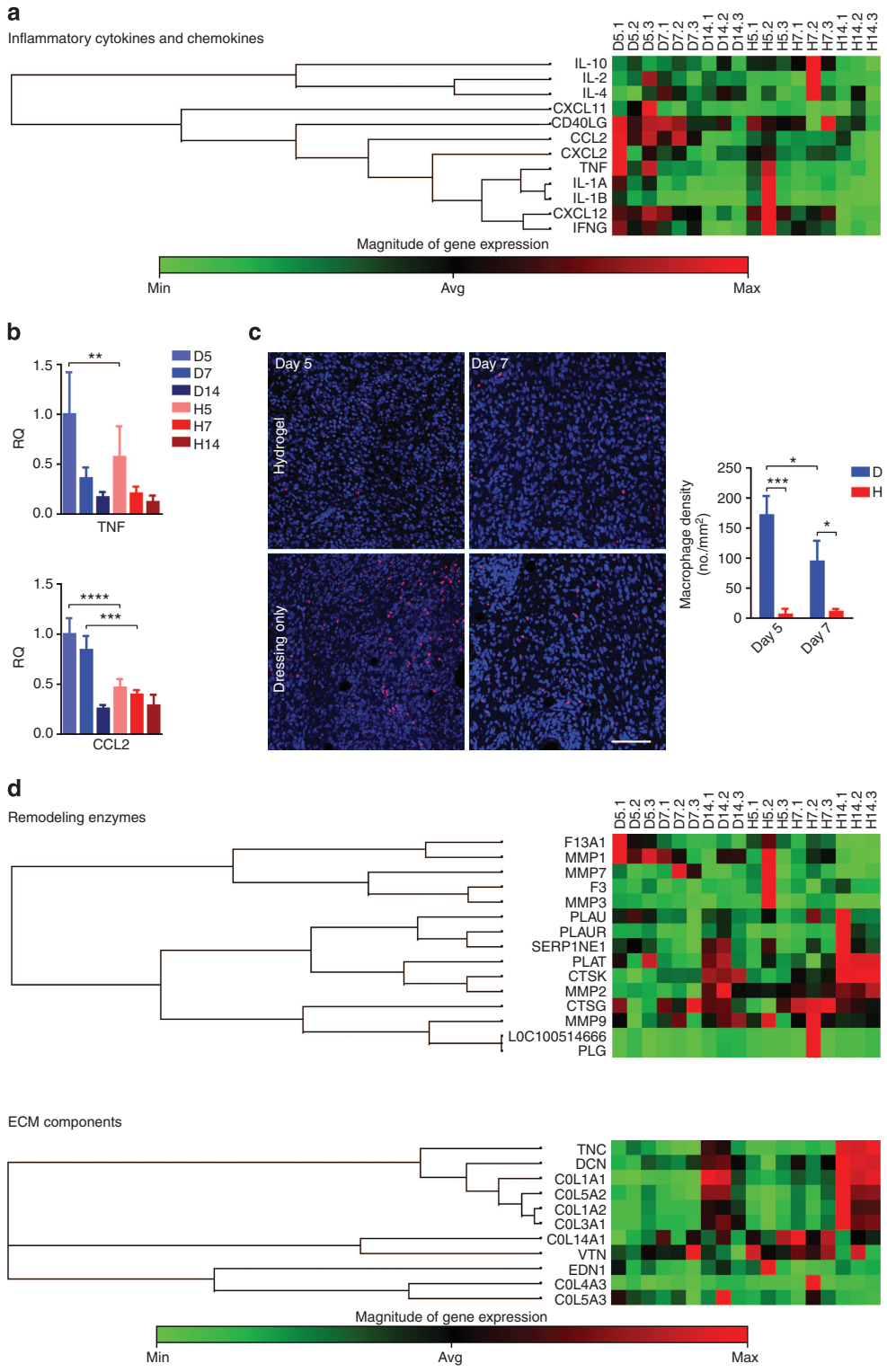

Figure 4. Healing kinetics. (**a**) Wound healing gene array analysis for inflammatory mediators on days 5,7, and 14. (**b**) Relative gene expression of tumor necrosis factor (TNF) and CCL2 of the treatments on days 5,7, and 14. (**c**, left panel) Representative images of immunofluorescence stain for macrophage (red; nuclei in blue) and (right panel) quantification of macrophage density in the wound area on days 5 and 7. (**d**) Wound healing gene array analysis for extracellular matrix (ECM)–associated genes on days 5, 7, and 14. Significance levels were set at $*P<0.05$, $**P<0.01$, and $***P<0.001$. D, dressing-only–treated wound; H, hydrogel-treated wound.

density from day 7 to day 14, whereas the dressing and dressing-re-treated group showed no significant change over the same time period (Supplementary Figure 2 online). On the basis of these results, the hydrogel treatment (without the retreating) procedure was used to continue our analyses of healing kinetics and remodeling.

Healing kinetics

To further analyze whether the dextran hydrogel–treated wounds heal in a more efficient manner, gene array analysis on days 5, 7, and 14 after treatment was performed. In general, we found that there was a higher expression of inflammatory mediators at day 5, suggestive of a stronger inflammatory response for the dressing-only–treated group, compared with that of hydrogel-treated wounds; this inflammatory response regressed over time (Figure 4a). Notably, expression analysis suggests that a persistence of inflammation may be driven by sustained expression of mediators such as chemokine (CCL2) and tumor necrosis factor in the dressing-treated wounds compared with hydrogel-treated wounds (Figure 4b). Immunostaining for macrophage marker (MAC387) revealed an abundance of macrophages throughout the granulation tissue at day 5 in the dressing-only–treated wounds, which decreased in density on day 7. In contrast, although macrophages were present in dextran hydrogel–treated wounds, significantly fewer macrophages were found in the granulation tissue in both time points (Figure 4c). In the meantime, hydrogel treatment induced expression of extracellular matrix (ECM) and remodeling genes compared with control (dressing-only–treated) wounds beginning at day 7 with differences maintained through day 14, suggesting superior granulation tissue formation (replacement of the hydrogel with native matrix and fibroblasts) and a more efficient remodeling of this matrix in hydrogel-treated wounds (Figure 4d). Overall, these results suggest that hydrogels, in comparison with treatment with dressing only, can promote a controlled healing response that is characteristic of a regenerative response, including efficient resolution of inflammation, promotion of an ECM–rich granulation tissue with accelerated vascular regression, and a superior rate of re-epithelialization and quality of neoepithelium formed.

Wound remodeling and re-innervation

To further examine the effect of hydrogel treatment on dermal remodeling, we analyzed dermal ECM protein composition at day 40 after treatment. We found that mature collagen fibers could be observed throughout the neodermis of hydrogel-treated wounds, whereas dressing-treated wounds had mature collagen fibers primarily at the periphery of the wounds, as evidenced by Masson's trichrome staining (Figure 5a and ci). Moreover, we found that elastic fibers were present in the periphery of hydrogel-treated wounds but were significantly reduced in dressing-treated wounds (Figure 5bi–ii and cii), suggesting that hydrogel-treated wounds were at a more advanced stage of remodeling compared with dressing-treated wounds at the same time.

In addition to significantly increased deposition of collagen and elastin fibers in hydrogel-treated wounds compared with controls, gene analysis revealed significant upregulation of KAL1 and laminin α2 mRNA expression (Figure 5d). These two genes are associated with neuron guidance (Blais *et al.*, 2009, 2013; Tengara *et al.*, 2010), indicating a potential greater peripheral neuron infiltration. Here, neuronal marker protein gene product 9.5 shows that, although both wound types have nerve fibers present at the edges of the wounds, peripheral nerve ingrowth to the central portion of the wounds was observed only in the hydrogel-treated wounds (Figure 5e).

DISCUSSION

Full- or split-thickness skin grafting is the current gold standard for wound closure following severe burn wound injury. A few synthetic substitutes have made their way to the market, but most provide only a temporary barrier until autografts are available for permanent closure (Supp, 2011). To the best of our knowledge, there is no synthetic product currently indicated for treating third-degree burns. We began by establishing a reproducible protocol for creating third-degree burn wounds in adult pigs. For third-degree burns in adult pigs, we found that 200 °C provides the sufficient heat for the wounds to progress into a full-thickness dermal damage within 48 hours. This progression of burn injury after initial heat damage is also seen in human burn patients (Nanney *et al.*, 1996).

Therefore, we theorized that treatment methods could impact the healing kinetics. In terms of treating the wounds with the dextran hydrogels, we found that completely excising the necrotic skin accelerated the infiltration of blood vessels into the treated areas and more profound regression of the neovessels over time, indicating better healing kinetics. On comparing dextran-based hydrogel treatment with the dressing-only–treated wounds, we found that wound closure was accelerated in dextran-based hydrogel-treated wounds, and the healing occurred in a regenerative manner, characterized by a rapid angiogenic response followed by vascular regression. Truly, angiogenesis followed by vessel regression has a crucial role in the wound healing progress (DiPietro, 2013; Hanjaya-Putra *et al.*, 2013), but compared with excisional wounds severe burn wounds exhibit impaired and slower neovascularization potentially because of delayed mobilization of circulating angiogenic cells (Zhang *et al.*, 2010; Hanjaya-Putra *et al.*, 2013; Guo *et al.*, 2014). Furthermore, rapid re-epithelialization and high quality of epithelium formed were present in the dextran-based hydrogel-treated wounds compared with control wounds. Even when the healing process was interfered with debridement, additional topical treatment with the hydrogel allowed fast re-epithelialization, demonstrating the robustness of the hydrogel treatment and its potential in the clinic. The rapid wound closure in the dextran-treated burns may be attributable to a combination of factors, including the moist environment provided by the hydrogels, which leads to a more efficient re-epithelialization and a faster stromal cell migration (Boateng *et al.*, 2008), excellent mechanical properties along with charged functional groups of the dextran hydrogel (Sun *et al.*, 2010), and the high angiogenic capability of the dextran hydrogel (Sun *et al.*,

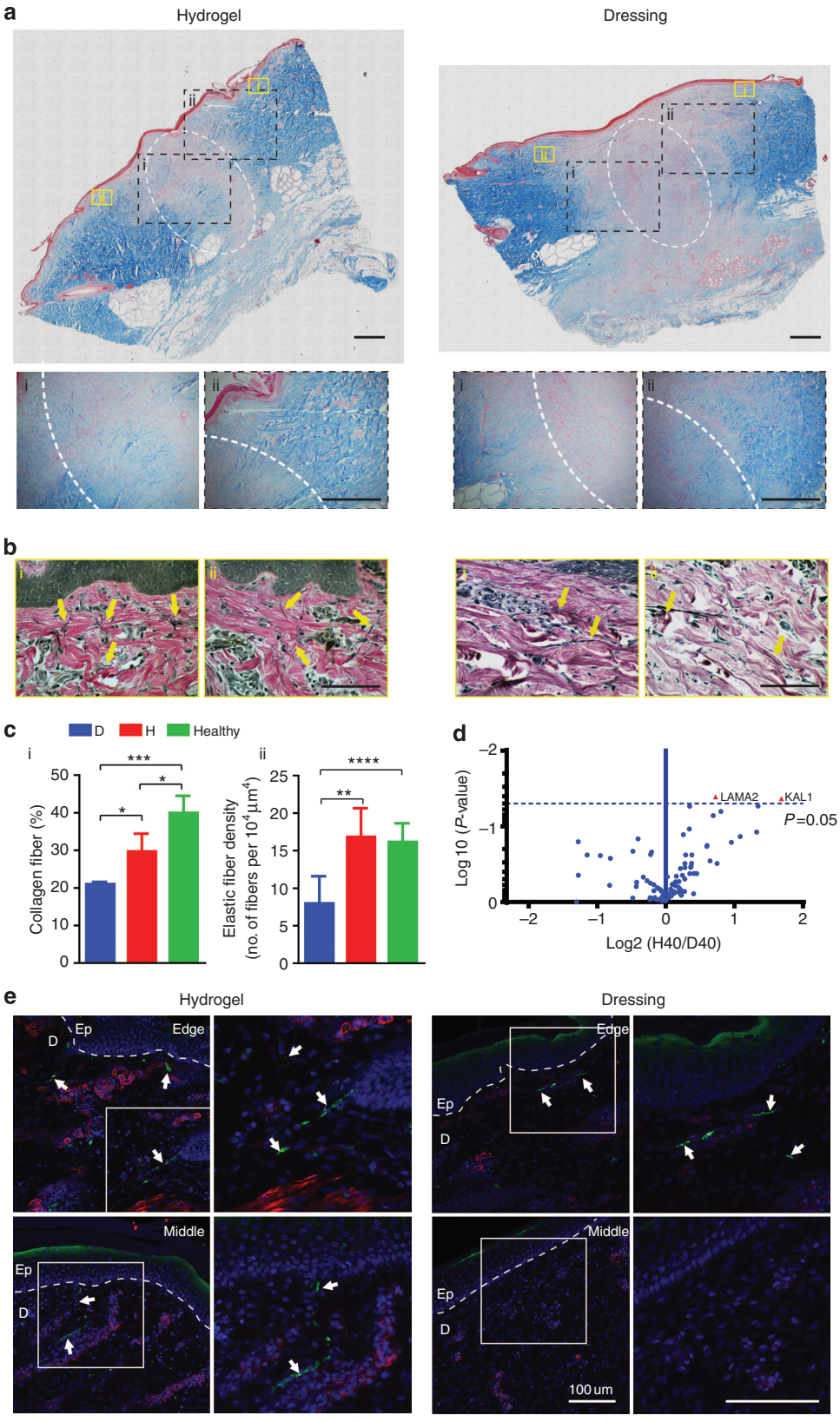
a
Hydrogel
Dressing
i
ii
b
c
D
H
Healthy
Collagen fiber (%)
Elastic fiber density (no. of fibers per 10^4 μm^4)
d
Log 10 (P-value)
Log2 (H40/D40)
LAMA2
KAL1
P=0.05
e
Hydrogel
Dressing
Ep
D
Edge
Middle
100 um

2010, 2011), all of which result in an overall quicker and better epidermis reconstruction.

The rapid onset and regression of the inflammatory response has a crucial role in coordinating the process of wound healing (Gurtner *et al.*, 2008). We found higher expression of proinflammatory mediators on day 5 in the dressing-treated wounds compared with the hydrogel-treated wounds, suggesting a persistent inflammatory response. Although the necessity of the inflammatory response in wound healing is debated (Ashcroft *et al.*, 1999; Martin *et al.*, 2003), in the context of biomaterial-induced healing, appropriate timings and durations of acute and chronic inflammatory responses would be needed for better healing results (Koh and DiPietro, 2011). Gene array analysis revealed lesser inflammatory response in the hydrogel-treated group than in the dressing-only–treated group. Immunohistochemistry showed high density of macrophages in the dressing-treated wounds on day 5, which regressed by day 7. In contrast, few macrophages in the dextran hydrogel–treated wounds could be observed during these time points. As inflammatory cells, especially macrophages, secrete essential cytokines and growth factors necessary for angiogenesis and stromal cell migration (Eming *et al.*, 2007), the elevated neovascularization followed by early vascular regression in the hydrogel-treated group strongly suggests earlier onset of the inflammatory response.

During the wound remodeling stage, the granulation tissue is being remodeled to reconstruct the loose regenerated dermis and strengthen the repaired tissue (Gurtner *et al.*, 2008). The severity of scarring depends on the amount and the organization of the secreted ECM during this phase. Therefore, an ideal skin substitute would induce high ECM deposition and organized crosslinking of ECM fibers to minimize scarring. Gene array analysis indicated that hydrogel treatment induced the expression of ECM and remodeling genes on days 7 and 14. Indeed, after 40 days of treatment, hydrogel-treated healing wounds showed a higher density of collagen compared with the dressing-only group, and the structure of the newly deposited collagen observed in the hydrogel-treated wounds showed higher organization. In addition, elastin fibers, which are usually poorly restored in scars (Lamme *et al.*, 1996), were deposited in higher density in hydrogel-treated wounds. Taken together with collagen, the regeneration of elastin provides favorable fiber frameworks for the later phase of wound healing (Eming *et al.*, 2007).

Because the skin is also a highly sensitive organ, after a deep burn injury, cutaneous nerves regenerate from the wound bed with the new nerve fiber migration or collateral sprouting from the adjacent skin (Blais *et al.*, 2013). In fact, burn victims often suffer permanent sensory deficits from abnormal sensation to chronic pain (Ward *et al.*, 1989; Ward and Tuckett, 1991; Malenfant *et al.*, 1996). As a result, neuron regeneration poses major challenges to improve patients' quality of life by restoring sensory perceptions to the regenerated skin. We found that dextran hydrogel treatment promoted nerve ingrowth into the regenerated skin, with the nerve fibers present close to the center of the wound on day 40. In contrast, we were unable to locate nerve fiber in the dressing-treated wounds. Combining our findings, the hydrogel treatment not only induced ECM remolding but also improved the re-innervation of the repaired wound. Further examination of the nerve fiber will be needed to identify the type and maturity of nerve fibers as well as the mechanism of the recruitment. Although we examined our samples, we found that these nerve fibers often time colocalized with the blood vessels. We thus speculate that perhaps the enhanced neovascularization during hydrogel treatment as well as more rapid re-epithelialization consequently contributed greater neural ingrowth during the healing progress.

It is important to note that the treatment groups used in our study are modeled on clinical care guidelines for third-degree burn wounds. Although the burn wound is completely excised in this model before hydrogel application, these wounds cannot be considered simple excisional wounds. Locally, edema develops even beyond the periphery of the excised tissue (as shown in Figure 1c). In addition, this model likely also captures the systemic hypermetabolic response, which is characteristic of third-degree burn injury that includes hyperinflammation, hormonal dysfunction, and catabolism (Jeschke *et al.*, 2007; Orgill, 2009; Williams *et al.*, 2009), although these parameters were not specifically examined in the current study. As such, these wounds differ from simple excisional wounds for local tumor removal or acute localized trauma. Given this systemic response to burn injury and the delay in excision, comparison of these wounds to simple excisional wounds in the same individual pig is invalid. Although the current study does not compare healing between this model and simple excisional wounds, future studies will explore the use of our hydrogels for other types of wounds, including acute injury models. Finally, whether the dextran-based hydrogel supports better healing compared with other commercially available hydrogels was not examined in this study.

Our study establishes a robust protocol for injury and hydrogel treatment of third-degree burns in a porcine large-animal model and thus paves the way for their use in clinical studies. The specific model was developed based on the surgical excision and grafting of full-thickness burn wounds that has been

Figure 5. Remodeling and reinnervation of third-degree burns. (**a**) Masson's trichome stain on day 40. High magnifications are the boxed areas. (**c**) (i) Quantification of collagen fiber % in the wounded area (indicated by the white dotted circle in **a**). (ii) Quantification of elastin fiber density in the dermis area adjacent to the epidermis. $N = 4$. (**b**) Representative images of Verhoeff–Van Gieson. With high magnification inset. Yellow arrows indicate mature elastin fibers. (**d**) Gene array analysis for wound remodeling. (**e**) Neuronal fibers (indicated by white arrows) at the edge of the wounds and in the middle of dressing-only–treated (right panel) and hydrogel-treated (left panel) wounds. Neurons (PGP9.5) in green, blood vessels (α-smooth muscle actin (SMA)) in red, and nuclei (4′,6-diamidino-2-phenylindole (Dapi)) in blue. Bar = 1 mm in **a** and 100 μm in **c** and **e**. Significance levels were set at $^{*}P < 0.05$, $^{**}P < 0.01$, $^{***}P < 0.001$, and $^{****}P < 0.0001$.

a common clinical practice for over 60 years (Cope *et al.*, 1947) and reflects current clinical guidelines (Jeschke *et al.*, 2013). Encouragingly, treating burned, full-thickness wounds with our dextran-based hydrogel allowed functional regeneration of the tissue through fast neovascularization and epithelial wound closure. In addition, the dextran hydrogel promotes more efficient dermis reconstruction and enhanced reinnervation. Overall, our findings support dextran-based hydrogels as an ideal candidate for the next generation of low-cost, off-the-shelf, and readily available treatment of a range of dermal injuries, which may enhance wound care for patients when skin autograft is neither available nor desirable.

MATERIALS AND METHODS

Hydrogel treatment and surgical procedure

The dextran hydrogel was synthesized and characterized as previously described (Sun *et al.*, 2010, 2011). *In vitro* cell toxicity was carried out using the WST assay (Sigma, St Louis, MO) and pilot *in vivo* mice tests (Sun *et al.*, 2011) to confirm the dextran hydrogel therapeutic properties.

Surgical procedures were approved by the Institutional Animal Care and Use Committee at Thomas D Morris (Reisterstown, MD) before the experiments. Two pigs were used to determine optimal wounding procedure and parameters for third-degree burn. Temperature was set at 100 °C and 200 °C while maintaining contact pressure at 2 kg cm^{-2} and contact duration of 30 seconds. Biopsy was taken 24 and 48 hours after injury for histological analysis. Three pigs were then used to investigate the therapeutic effect of dextran hydrogel on burn wounds. Following injury, the wounds were left for 48 hours for stabilization before the excision procedure. A total of 70 circular third-degree burn wounds (1.2 or 1.5 cm in diameter) were created. Circular biopsy punches were used for partial or complete excision for full-thickness wound down to the necrotic adipose layer. Wounds were at least 3 cm apart from one another to minimize hindered wound healing process due to proximity. After the excision procedure, wounds were cleaned with sterile gauze to temporarily stop bleeding. Half of the wounds were treated with dextran hydrogel and the other half were left untreated. Treated and untreated wounds were first sealed with Tegaderm (3M, St Paul, MN) and compound benzoin tincture (Medical Chemical Corp, Torrence, CA) to enhance the Tegaderm adherence to the skin. An additional layer of Vetrap (3M) and an elastic body suit (VetMedCare, Koblach, Austria) were worn over the body. To protect the newly forming epidermis from traumatization during bandage change, a non-adhesive Curity dressing (Covidien, Minneapolis, MN) was placed under the Tegaderm layer. After wound closure, only an elastic body suit was worn over the wounds. For retreatment, redebridement was made, and a new half the thickness hydrogel was placed on top for retreatment. Secondary excision was made on control group, as well for the retreatment group. Dressings were changed three times a week until wound closure was complete. This dressing procedure as well as maintenance conditions were consistent between pigs throughout the duration of the experiments.

Healing evaluation

Blood flow was monitored noninvasively using moorFLPI speckle contrast imager (Moor Instruments, Wilmington, DE). The measurements were normalized by the blood flow measurements of the healthy skin area adjacent to each wound.

For immunohistochemical assay, collected skin specimens were fixed and embedded in paraffin. Bisected wounds were sectioned serially to ensure analysis of the mid-point of the wounds, as described previously (Swift *et al.*, 2001). Histologic sections were stained with hematoxylin and eosin, Masson's trichrome, and Verhoeff–van Gieson's stain or immunohistochemistry for CD31, cytokeratin 14, MAC387 (all from Abcam, Cambridge, MA), SMA (α-smooth muscle actin) (Dako, Carpinteria, CA), Dapi (4',6-diamidino-2-phenylindole), PGP9.5 (AbD Serotec, Kidlington, UK), and matching AlexaFlour secondary (Life Technologies, Grand Island, NY). Histological images were taken with upright light microscope and camera (Nikon, Melville, NY). Full-specimen images were scanned using automated motor controlled Nikon T1 and tiled together with corresponded software (Nikon Nis-Element, Melville, NY). Fluorescent images were taken with confocal (Zeiss LSM780, Oberkochen, Germany). The area and the number of vessels inside the wounds were quantified from CD31-stained sections using the ImageJ software (National Institutes of Health, Bethesda, MD) as described previously (Sun *et al.*, 2011; Hanjaya-Putra *et al.*, 2013). Wound gap area was measured photometrically. Re-epithelialization was calculated as the percentage of regenerated epithelium (K14 positive) of the entire wound. Maturation of the re-epithelialization was quantified by rete ridge formation density as described previously (Kiwanuka *et al.*, 2011). Collagen fiber deposition was quantified from Masson's trichrome images by calculating the percentage of collagen fiber presented in the wound. Using the ImageJ software, we quantified the percentage of stained collagen fibers in the given area in each group. Elastin fibers were quantified from Verhoeff–van Gieson's stain across the dermis area adjacent to the epidermis similarly to the collagen. Nerve innervation analysis was performed on a 25 μm paraffin sections on gelatin-coated slides. Slides were then analyzed in confocal using serial z-stack imaging.

Gene expression analysis was performed using two-step reverse transcription-PCR on wound specimens in accordance with the manufacturer instructions (Applied Biosystems, Grand Island, NY). Wound healing and ECM reverse transcription-PCR array sets (Qiagen, Valencia, CA) were used to compare the expression profile. For each primer, the comparative computerized method provided by the manufacturer was used to calculate the amplification differences between different samples.

Statistical analysis

For wounding parameter determination two pigs were used. For wound healing analysis, a total of three pigs with $n > 12$ wounds for each condition with at least $n = 3$ for each time point detailed throughout the manuscript. For quantification of blood vessels and re-epithelialization, whole wounds were analyzed as detailed above. Real-time reverse transcription-PCR was performed on triplicate samples ($n = 3$) with triplicate readings. Statistic was calculated by the computerized method provided by the manufacturer to obtain *P*-value of the gene expression. For data presentation, relative gene expression was graphed with relative fold change of the targeted group/dressing day 5. For all other assays, statistical analysis was performed using the GraphPad Prism 6.01 (GraphPad Software, La Jolla, CA) to perform *t*-tests, one-way analysis of variance with Turkey's post-test, or two-way analysis of variance with Bonferroni's post-test where appropriate. Significance levels were set at $^*P < 0.05$,

$^{**}P<0.01$, $^{***}P<0.001$, and $^{****}P<0.0001$. Unless otherwise indicated, all graphical data are reported ± SD.

CONFLICT OF INTEREST

Intellectual property related to the hydrogel technology is owned by Johns Hopkins University and licensed to Gemstone Biotherapeutics LLC of which SG is a cofounder, consultant, and director. SG has a financial interest in Gemstone Biotherapeutics LLC, which is subject to certain restrictions under University policy. The terms of this arrangement are being managed by the Johns Hopkins University in accordance with its conflict of interest policies. SWV received fees for service consulting for Gemstone Biotherapeutics LLC. Gemstone Biotherapeutics LLC did not affect the design, interpretation, or reporting of any of the experiments herein. Y-IS, H-HGS, AP, and JB report that they have no competing interests. *Data and materials availability*: Hydrogel technology described here can be synthesized from commercially available materials as described in Materials and Methods section. Depending on availability, hydrogels can be transferred upon request to other academic researchers using letter agreements that conform to the intent of the Material Transfer Agreement (MTA).

ACKNOWLEDGMENTS

We thank Markus Tammia and Dr Hai-Quan Mao for assistance with neuronal stain. This work was supported by Gemstone Biotherapeutics LLC and NIH grant R01HL107938 (to SG).

AUTHOR CONTRIBUTIONS

Y-IS and H-HGS: Designed and performed research, analyzed data, and wrote the paper; AP and JB: analyzed data; SWV: analyzed data and wrote the paper; and SG: designed research, analyzed data, and wrote the paper.

SUPPLEMENTARY MATERIAL

Supplementary material is linked to the online version of the paper at http://www.nature.com/jid

REFERENCES

Ashcroft GS, Yang X, Glick AB *et al.* (1999) Mice lacking Smad3 show accelerated wound healing and an impaired local inflammatory response. *Nat Cell Biol* 1:260–6

Blais M, Grenier M, Berthod F (2009) Improvement of nerve regeneration in tissue-engineered skin enriched with schwann cells. *J Invest Dermatol* 129: 2895–900

Blais M, Parenteau-Bareil R, Cadau S *et al.* (2013) Concise review: tissue-engineered skin and nerve regeneration in burn treatment. *Stem Cells Transl Med* 2:545–51

Boateng JS, Matthews KH, Stevens HN *et al.* (2008) Wound healing dressings and drug delivery systems: a review. *J Pharmaceut Sci* 97:2892–923

Branski LK, Mittermayr R, Herndon DN *et al.* (2008) A porcine model of full-thickness burn, excision and skin autografting. *Burns* 34:1119–27

Cope O, Langohr JL, Moore FD *et al.* (1947) Expeditious care of full-thickness burn wounds by surgical excision and grafting. *Ann Surg* 125:1

DiPietro LA (2013) Angiogenesis and scar formation in healing wounds. *Curr Opin Rheumatol* 25:87–91

Eming SA, Krieg T, Davidson JM (2007) Inflammation in wound repair: molecular and cellular mechanisms. *J Invest Dermatol* 127:514–25

Gaines C, Poranki D, Du W *et al.* (2013) Development of a porcine deep partial thickness burn model. *Burns* 39:311–9

Guo R, Teng J, Xu S *et al.* (2014) Comparison studies of the *in vivo* treatment of full-thickness excisional wounds and burns by an artificial bilayer dermal equivalent and J-1 acellular dermal matrix. *Wound Rep Regen* 22:390–8

Gurtner GC, Werner S, Barrandon Y *et al.* (2008) Wound repair and regeneration. *Nature* 453:314–21

Hanjaya-Putra D, Shen Y-I, Wilson A *et al.* (2013) Integration and regression of implanted engineered human vascular networks during deep wound healing. *Stem Cells Transl Med* 2:297–306

Hop MJ, Polinder S, van der Vlies CH *et al.* (2014) Costs of burn care: a systematic review. *Wound Rep Regen* 22:436–50

Jeschke MG, Finnerty CC, Suman OE *et al.* (2007) The effect of oxandrolone on the endocrinologic, inflammatory, and hypermetabolic responses during the acute phase postburn. *Ann Surg* 246:351–60

Jeschke MG, Kamolz L, Shahrokhi S (2013) *Burn Care and Treatment: A Practical Guide*. Springer: Vienna, Austria

Kiwanuka E, Hackl F, Philip J *et al.* (2011) Comparison of healing parameters in porcine full-thickness wounds transplanted with skin micrografts, split-thickness skin grafts, and cultured keratinocytes. *J Am Coll Surg* 213: 728–35

Koh TJ, DiPietro LA (2011) Inflammation and wound healing: the role of the macrophage. *Expert Rev Mol Med* 13:e23

Lamme EN, de Vries HJ, van Veen H *et al.* (1996) Extracellular matrix characterization during healing of full-thickness wounds treated with a collagen/elastin dermal substitute shows improved skin regeneration in pigs. *J Histochem Cytochem* 44:1311–22

Malenfant A, Forget R, Papillon J *et al.* (1996) Prevalence and characteristics of chronic sensory problems in burn patients. *Pain* 67:493–500

Martin P, D'Souza D, Martin J *et al.* (2003) Wound healing in the PU.1 null mouse—tissue repair is not dependent on inflammatory cells. *Curr Biol* 13: 1122–8

Middelkoop E, van den Bogaerdt AJ, Lamme EN *et al.* (2004) Porcine wound models for skin substitution and burn treatment. *Biomaterials* 25: 1559–67

Nanney LB, Wenczak BA, Lynch JB (1996) Progressive burn injury documented with vimentin immunostaining. *J Burn Care Res* 17:191–8

Orgill DP (2009) Excision and skin grafting of thermal burns. *N Engl J Med* 360: 893–901

Papp A, Kiraly K, Härmä M *et al.* (2004) The progression of burn depth in experimental burns: a histological and methodological study. *Burns* 30: 684–90

Sheridan RL (2012) *Burns: A Practical Approach to Immediate Treatment and Long-Term Care*. Manson Publishing: London, UK

Singer AJ, McClain SA (2003) A Porcine Burn Model. In: *Wound Healing: Methods and Protocols* 78:107–19

Stoddard FJ Jr., Ryan CM, Schneider JC (2014) Physical and psychiatric recovery from burns. *Surg Clin N Am* 94:863–78

Sullivan TP, Eaglstein WH, Davis SC *et al.* (2001) The pig as a model for human wound healing. *Wound Rep Regen* 9:66–76

Sun G, Shen YI, Ho CC *et al.* (2010) Functional groups affect physical and biological properties of dextran-based hydrogels. *J Biomed Mater Res Part A* 93:1080–90

Sun G, Zhang X, Shen YI *et al.* (2011) Dextran hydrogel scaffolds enhance angiogenic responses and promote complete skin regeneration during burn wound healing. *Proc Natl Acad Sci USA* 108:20976–81

Supp DM (2011) Skin substitutes for burn wound healing: current and future approaches. *Informa Healthcare* 6:217–27

Swift ME, Burns AL, Gray KL *et al.* (2001) Age-related alterations in the inflammatory response to dermal injury. *J Invest Dermatol* 117:1027–35

Tengara S, Tominaga M, Kamo A *et al.* (2010) Keratinocyte-derived anosmin-1, an extracellular glycoprotein encoded by the X-linked Kallmann syndrome gene, is involved in modulation of epidermal nerve density in atopic dermatitis. *J Dermatol Sci* 58:64–71

Ward RS, Saffle JR, Schnebly WA *et al.* (1989) Sensory loss over grafted areas in patients with burns. *J Burn Care Rehabil* 10:536–8

Ward RS, Tuckett RP (1991) Quantitative threshold changes in cutaneous sensation of patients with burns. *J Burn Care Rehabil* 12:569–75

Williams FN, Jeschke MG, Chinkes DL *et al.* (2009) Modulation of the hypermetabolic response to trauma: temperature, nutrition, and drugs. *J Am Coll Surg* 208:489–502

Zhang X, Wei X, Liu L *et al.* (2010) Association of increasing burn severity in mice with delayed mobilization of circulating angiogenic cells. *Archiv Surg* 145:259–66